

Article

Experimental Study and Mathematical Modeling of Mechanical Properties of Basalt Fiber-Reinforced Recycled Concrete Containing a High Content of Construction Waste

Wei-Zhi Chen and Xue-Fei Chen * 

Joint Key Laboratory of the Ministry of Education, Institute of Applied Physics and Materials Engineering, University of Macau, Avenida da Universidade, Taipa, Macau 999078, China; weizhichen@gzhu.edu.cn

* Correspondence: chenxuefei@email.szu.edu.cn

Abstract: Herein, we conducted an experimental test on basalt fiber-reinforced concrete with a high content of construction and demolition waste and then established some mathematical models based on Taylor's formula. The concrete was prepared by using recycled clay brick powder in place of cement and recycled coarse aggregates as a substitution for natural coarse aggregates. The basalt fiber in weight dosages of 0, 0.1, 0.3, and 0.5% was used for reinforcement. The results showed that the compressive strength of concrete declined as the content of recycled aggregates increased, while the compressive strength first increased and then decreased as the basalt fiber dosage lifted. Regarding the splitting tensile strength, the reinforcement effect of basalt fiber in concrete with a high content of recycled aggregate is more significant when compared to its counterpart, which contains no or fewer recycled aggregates. The concrete with 0.5% basalt fiber dosage and 100% recycled aggregate content retains an equivalent compressive strength as to that of natural aggregate concrete and has about a 90% splitting tensile strength. In addition, the cubic function in comparison to the quadratic function has a higher fitting accuracy.

Keywords: concrete; recycled aggregates; construction waste



Citation: Chen, W.-Z.; Chen, X.-F. Experimental Study and Mathematical Modeling of Mechanical Properties of Basalt Fiber-Reinforced Recycled Concrete Containing a High Content of Construction Waste. *Constr. Mater.* **2023**, *3*, 462–473. <https://doi.org/10.3390/constrmater3040030>

Received: 7 September 2023

Revised: 18 October 2023

Accepted: 24 November 2023

Published: 28 November 2023



Copyright: © 2023 by the authors. Licensee MDPI, Basel, Switzerland. This article is an open access article distributed under the terms and conditions of the Creative Commons Attribution (CC BY) license (<https://creativecommons.org/licenses/by/4.0/>).

1. Introduction

The global use of concrete has exceeded 4 billion m³/year, and the use of sand and gravel materials has exceeded 6 billion to 8 billion tons/year [1,2]. Mining is used to satisfy such a large demand for sand and aggregates. However, mining consumes many natural resources and causes environmental pollution and ecological damage [3–5]. In addition, the demolition of old houses, factories, and other buildings for various reasons generates a large amount of waste concrete. The annual production of construction and demolition waste in China reaches 1.8 billion tons and is increasing year by year [6–8]. The most common practice at present to treat waste concrete is to pile it up or place it in landfills [9–12].

The mining method not only occupies a large land resource but also causes environmental pollution. On the contrary, waste concrete can be crushed and ground to obtain recycled aggregate, which can be partially or completely replaced by recycled aggregate to prepare recycled concrete as per previous research [13,14]. To a certain extent, it alleviates the pressure of natural aggregate extraction and solves the land occupation and environmental pollution problems caused by waste concrete, thus realizing the green and sustainable development of waste concrete [15–17]. However, compared with natural aggregates, waste concrete aggregates have the disadvantages of high water absorption, high porosity, low apparent density, and a high crushing value, resulting in the low strength and poor durability of the prepared recycled concrete. Therefore, it is crucial to improve the performance of recycled concrete [18–20].

Researchers have delved into two primary approaches for modifying recycled aggregates, aiming to ameliorate their detrimental impact on new concrete. The first approach involves employing biological, chemical, and mechanical techniques [21–24], among others, to mitigate the adverse effects of the recycled aggregate's subpar quality. This includes strategies like eliminating the residual adhesive mortar from the aggregate's surface and enhancing the adhesive mortar's performance. The second approach entails enhancing the overall quality of synthesized recycled concrete directly by incorporating supplementary materials, such as polymers and mineral admixtures [25–30]. Heat treatment stands out as a favorable approach for dissolving weakly bonded mortar because of its straightforward application and cost efficiency. However, this method is contrary to the low-carbon objective, as it triggers additional energy consumption. An alternative method, mechanical treatment, is widely employed in detaching bonded mortar from the original natural aggregate, yielding premium recycled aggregate [19]. This technique employs mechanical force to crush and dislodge the bonding mortar. Yet, given the collision and grinding inherent in the process, there is a propensity for detrimental impacts on the structural integrity of recycled aggregate particles. This may lead to alterations in the geometric attributes of these particles, thereby potentially introducing new microcracks [31–34]. Subsequently, acid prepreg technology was developed; it has the ability to effectively improve the quality of recycled aggregates by eliminating bonding mortar. However, usually after treatment with hydrochloric or sulfuric acid, the chloride and sulfate content of the aggregate will increase, which, in turn, affects the durability of the concrete. In recent years, there is more and more research on carbonization to improve the properties of recycled aggregates because carbonization can increase the density of cementified materials. Liang et al. [35] studied the carbonization behavior of concrete containing carbonized recycled aggregate in different environments, and the results showed that a CO₂ curing treatment improved the physical and chemical properties of recycled aggregate (such as significantly reducing the water absorption of RA). The recycled concrete prepared by adding carbonized fine and coarse recycled aggregate has higher compressive strength and lower carbonization depth, and the carbonization depth decreases more obviously [36–38].

Other enhancements involve using various fibers, such as steel fibers, polyvinyl alcohol fibers, carbon fibers, and so forth, to improve the strength and toughness of recycled concrete [39–41]. Steel fibers have a strengthening and toughening effect on recycled aggregates, but they are heavy. Carbon fiber is expensive. Basalt fiber, as a kind of green material, has a high tensile strength, a high modulus of elasticity, a low price, and enhanced toughening [16,42–44]. Basalt fiber has thereby recently been considered a potential reinforcement material to strengthen concrete prepared by recycled aggregates. Li et al. [45] studied the influence of different fiber contents on the mechanical properties of fiber-reinforced concrete (HFRC), especially the shear strength and toughness, and obtained the optimal fiber content in HFRC. The results show that the compressive strength of HFRC is higher than that of plain concrete when the content of basalt fiber is less than 0.15%. Algin and Ozen et al. [46] studied the application of basalt fiber in the production of self-compacting concrete (SCC) to determine the influence of fiber addition on the working and mechanical properties of concrete. The results show that, when the fiber length is 12 mm and the fiber content is 0.1%, the compressive strength can be improved. At present, most studies consider only the length of fiber or the content of fiber and other single factors for fiber-reinforced recycled concrete. It is necessary to use basalt fiber with different contents (0.1~0.3%) and different lengths (6~18 mm) to determine the optimum content and length of fiber. It is necessary to consider the influence of many factors on the slump, compressive strength, splitting tensile strength, and bending strength of recycled concrete. Zhang et al. [42] first proposed the composite effect based on the fiber reinforcement theory. The effects of the mixture of the regenerated coarse aggregate replacement rate and BF content on the failure mode, mechanical properties, and interfacial transition zone properties of regenerated concrete were studied by conducting a macroscopic performance analysis and microscopic test. The results show that the basic mechanical properties of

recycled concrete with different BF contents are better than ordinary concrete when the replacement rate of recycled aggregate is 50%.

We conducted an experimental study on the basalt fiber-reinforced recycled aggregate concrete. The novelty lies in the use of a mathematical model established by the Taylor formula and the associated surface trend map in analysis.

2. Experimental Details

2.1. Materials

The binding materials are ordinary Portland cement with grade P.O.42.5 and recycled clay brick powder (RCBP) with an average particle size of 20 μm . Fine aggregate with a size of less than 4.75 mm is common river sand. Coarse aggregates with a size between 4.75 and 19.5 mm contain both natural aggregates (NAs) and recycled aggregates (RAs). Polycarboxylate superplasticizer was used as the water reducer to control the fluidity of fresh concrete. The chemical composition and physical properties of the raw materials are listed in Tables 1–3, respectively. Figure 1 shows the in-site photos of coarse aggregates and fibers.

Table 1. Chemical composition of cement and recycled clay brick powder (RCBP) (%).

	SiO ₂	Fe ₂ O ₃	Al ₂ O ₃	CaO	MgO	SO ₃	Na ₂ O	K ₂ O	LOI
Cement	21.58	3.36	5.62	61.31	2.32	2.41	0	0	3.40
RCBP	49.02	6.97	31.56	4.88	0.83	0	1.05	0.73	5.79

Table 2. Physical properties of aggregates.

Type	Apparent Density (kg/cm ³)	Bulk Density (kg/cm ³)	Water Absorption (%)	Fineness Modulus (Mx)
Natural fine aggregate	2640	1490	0.98	2.83
Natural coarse aggregate	2840	1730	0.52	-
Recycled coarse aggregate	2630	1550	3.87	-

Table 3. Physical properties of basalt fiber.

Length/mm	Diameter/ μm	Density (g/cm ³)	Modulus of Elasticity/GPa	Tensile Strength/MPa
18	15	2.64	110	4800



Figure 1. In-site photos of raw materials: NAs, natural coarse aggregates (left); RAs, recycled coarse aggregates (middle); BF, basalt fiber (right).

2.2. Sample Preparation

The cement, aggregates, and fibers were first dry-mixed for about 3 min and then wet-mixed with water for another 3 min. RAs were pre-wetted to reach the saturated surface dry status to avoid the reduction of free water available for cement hydration. The initial slump value was controlled at 160–180 mm by adding various dosages of water reducers, with the specific mix. proportion exhibited in Table 4. Fresh samples were poured into 100 mm cubic steel molds to generate the initial strength, whilst the hardened specimens were transferred to the standard curing chamber (temp. c.a. 25 °C, RH > 95%) and cured for 28 days.

Table 4. Mix. proportion of samples.

Notation	RA Content wt. %	BF Dosage wt. %	Cement (kg/m ³)	RCBP (kg/m ³)	Water (kg/m ³)	Sands (kg/m ³)	NA (kg/m ³)	RA (kg/m ³)	Water Reducer (kg/m ³)	BF (kg/m ³)
1 (Control)	0	0	347.2	86.8	210	708	1061	0	1.77	0.0
2	20	0	347.2	86.8	210	708	849	212	1.77	0.0
3	30	0	347.2	86.8	210	708	743	318	1.79	0.0
4	40	0	347.2	86.8	210	708	637	424	1.81	0.0
5	50	0	347.2	86.8	210	708	531	531	1.82	0.0
6	60	0	347.2	86.8	210	708	424	637	1.83	0.0
7	80	0	347.2	86.8	210	708	212	849	1.86	0.0
8	100	0	347.2	86.8	210	708	0	1061	2.00	0.0
9	0	0.1	347.2	86.8	210	708	1061	0	1.79	0.4
10	20	0.1	347.2	86.8	210	708	849	212	1.88	0.4
11	30	0.1	347.2	86.8	210	708	743	318	1.91	0.4
12	40	0.1	347.2	86.8	210	708	637	424	1.92	0.4
13	50	0.1	347.2	86.8	210	708	531	531	1.94	0.4
14	60	0.1	347.2	86.8	210	708	424	637	2.02	0.4
15	80	0.1	347.2	86.8	210	708	212	849	2.03	0.4
16	100	0.1	347.2	86.8	210	708	0	1061	2.24	0.4
17	0	0.3	347.2	86.8	210	708	1061	0	2.02	1.3
18	20	0.3	347.2	86.8	210	708	849	212	2.02	1.3
19	30	0.3	347.2	86.8	210	708	743	318	2.15	1.3
20	40	0.3	347.2	86.8	210	708	637	424	2.15	1.3
21	50	0.3	347.2	86.8	210	708	531	531	2.16	1.3
22	60	0.3	347.2	86.8	210	708	424	637	2.21	1.3
23	80	0.3	347.2	86.8	210	708	212	849	2.27	1.3
24	100	0.3	347.2	86.8	210	708	0	1061	2.37	1.3
25	0	0.5	347.2	86.8	210	708	1061	0	2.05	2.2
26	20	0.5	347.2	86.8	210	708	849	212	2.21	2.2
27	30	0.5	347.2	86.8	210	708	743	318	2.24	2.2
28	40	0.5	347.2	86.8	210	708	637	424	2.25	2.2
29	50	0.5	347.2	86.8	210	708	531	531	2.29	2.2
30	60	0.5	347.2	86.8	210	708	424	637	2.31	2.2
31	80	0.5	347.2	86.8	210	708	212	849	2.41	2.2
32	100	0.5	347.2	86.8	210	708	0	1061	2.46	2.2

2.3. Testing and Modeling

The compressive strength and the splitting tensile strength of basalt fiber-reinforced recycled aggregate concrete were determined by a universal machine (HYE-300), and the load rates were set as 0.1 MP/s and 0.01 MP/s, respectively. The mathematical model was established based on Taylor’s formula, which hypothesizes that all functions can be approximated by polynomials with various orders.

3. Results and Discussion

3.1. Compressive Strength

Figure 2 illustrates the experimental and modeled results of the compressive strength of concrete with various recycled aggregate contents and basalt fiber dosages. The circles in Figure 2a indicate the experimental results, while the surface trend is modeled by a cubic

polynomial incorporating two variables, namely the content of recycled aggregate and the dosage of basalt fiber. The cubic polynomial is shown in the following equation.

$$f_c = b_{21} + b_{22} * X + b_{23} * Y + b_{24} * X * Y + b_{25} * X.^2 + b_{26} * Y.^2 + b_{27} * Y * X.^2 + b_{28} * X * Y.^2 + b_{29} * X.^3 + b_{210} * Y.^3 \quad (1)$$

where X indicates the matrix of recycled aggregate, and Y indicates the matrix of basalt fiber.

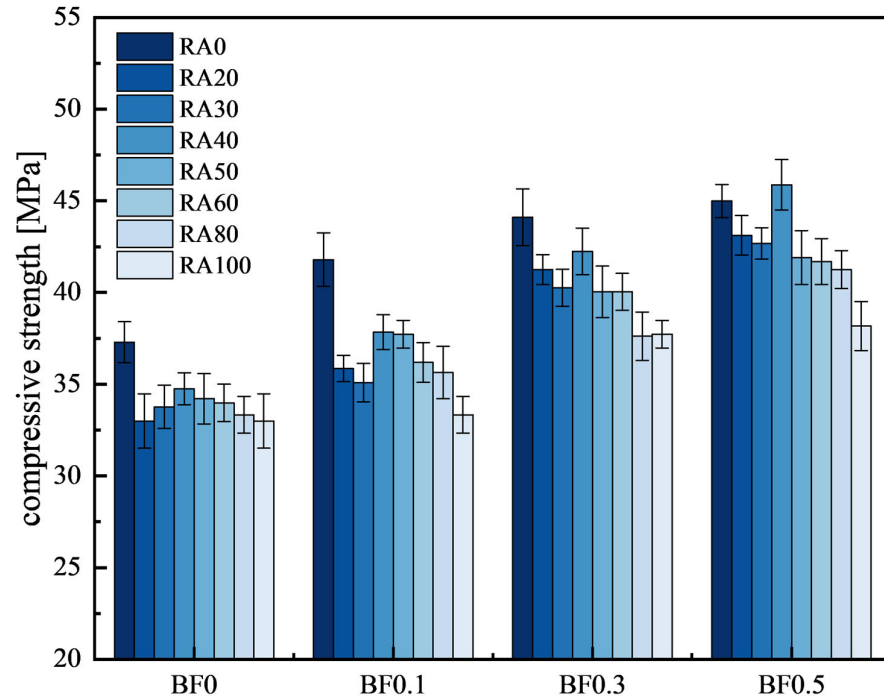


Figure 2. Compressive strength of basalt fiber-reinforced recycled concrete.

The matrix of parameters accommodating b_{2i} ($i = 1-10$) is shown in Table 5.

Table 5. Parameter matrix of the fitted cubic polynomial of the compressive strength.

b21	b22	b23	b24	b25	b26	b27	b28	b29	b210
37.19	-0.21	33.94	-0.01	0.00	-36.46	0.00	0.30	0.00	1.60

Figure 2 map the absolute value of deviations between the experimental results and fitted results. The depth of color is directly proportional to the absolute value of deviation. It is observed that the majority of the deviation is less than 5%, indicating the good fitting performance of the cubic model.

As shown in Figures 2 and 3, the compressive strength of ordinary concrete with 0.1% basalt fiber is lower than that of concrete without fiber. However, with the increase in the basalt fiber dosage, its compressive strength increases, and when the basalt fiber dosage reaches 0.3%, the compressive strength exceeds that of the unadulterated fiber concrete by 5.8%. Thus, it can be seen that a larger amount of basalt fibers for an ordinary concrete enhancement effect is more obvious. For concrete specimens with the same replacement rate of recycled coarse aggregate, the compressive strength decreased with the increase in basalt fibers at 0.1% and 0.3% of basalt fiber dosage but showed a stable increase with the increase in the recycled coarse aggregate replacement rate at the same fiber dosage, and the increasing trend was obvious at 0.1% of fiber dosage. However, for the 0.5% fiber dosage, the compressive strength of specimens fluctuated greatly, first showing a decline, then a rise, and then a decline, and in the recycled coarse aggregate substitution rate of 40%, the compressive strength reached the maximum, and even more than 10% of the compressive

strength of ordinary concrete. With the fiber doping at 0.3% and the 40% replacement rate of recycled coarse aggregate, the concrete reached the maximum compressive strength.

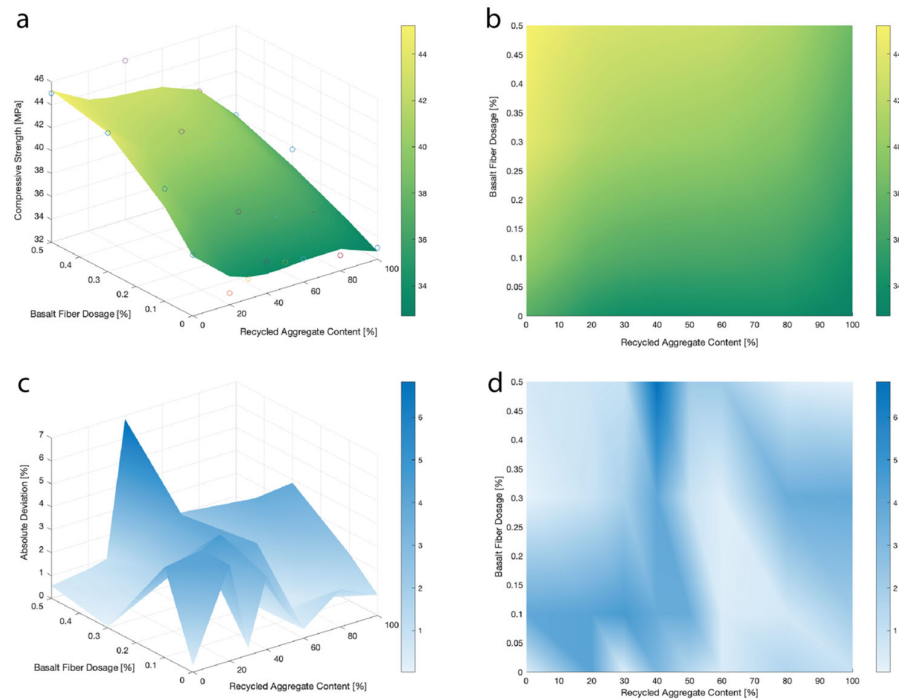


Figure 3. Compressive strength: (a) 3D trend surface of compressive strength, (b) contour map of compressive strength, (c) 3D distribution of absolute deviation, and (d) contour map of absolute deviation.

First, basalt fiber has a larger specific surface area and a higher friction coefficient [15], increasing the relative friction of the concrete mix and increasing the bond between the fiber and the cement matrix. Second, the density of basalt fibers and the density of concrete are very similar to that of the concrete, resulting in better compatibility with the concrete [47]. Thirdly, basalt fibers can increase the water retention of concrete, and it was pointed out that basalt fibers can effectively prevent the segregation of concrete so that the cohesion and water retention of concrete is improved. However, since basalt concrete specimens are mainly stressed by coarse aggregates, and basalt fibers absorb a large amount of water during mixing, the recycled concrete at a larger replacement rate cannot be fully hydrated, resulting in a reduction in strength [48]. Therefore, 0.3% basalt fibers had the most significant effect on the compressive strength of concrete specimens with a 40% replacement of recycled coarse aggregate.

3.2. Splitting Tensile Strength

Figures 4 and 5 illustrate the profile of the splitting tensile strength, and they are depicted by the quadratic and the cubic mathematical model, respectively. It is noted that the cubic model has a higher fitting accuracy in comparison to the quadratic model, with visual differences being present between Figures 3d and 4d.

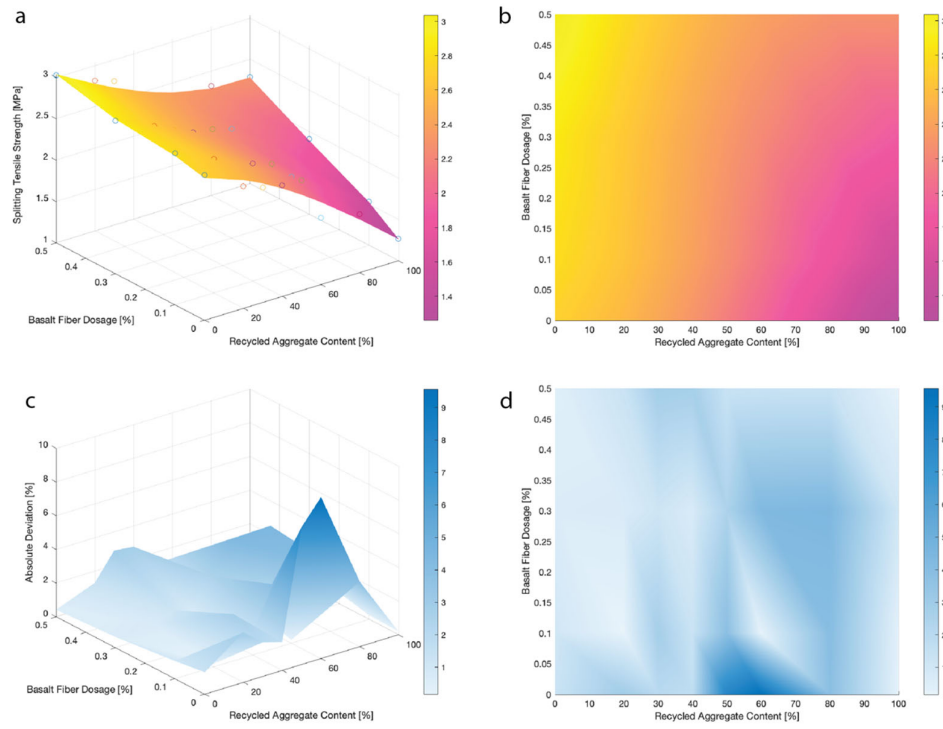


Figure 4. Splitting tensile strength with quadratic function: (a) 3D trend surface of splitting tensile strength, (b) contour map of splitting tensile strength, (c) 3D distribution of absolute deviation, and (d) contour map of absolute deviation.

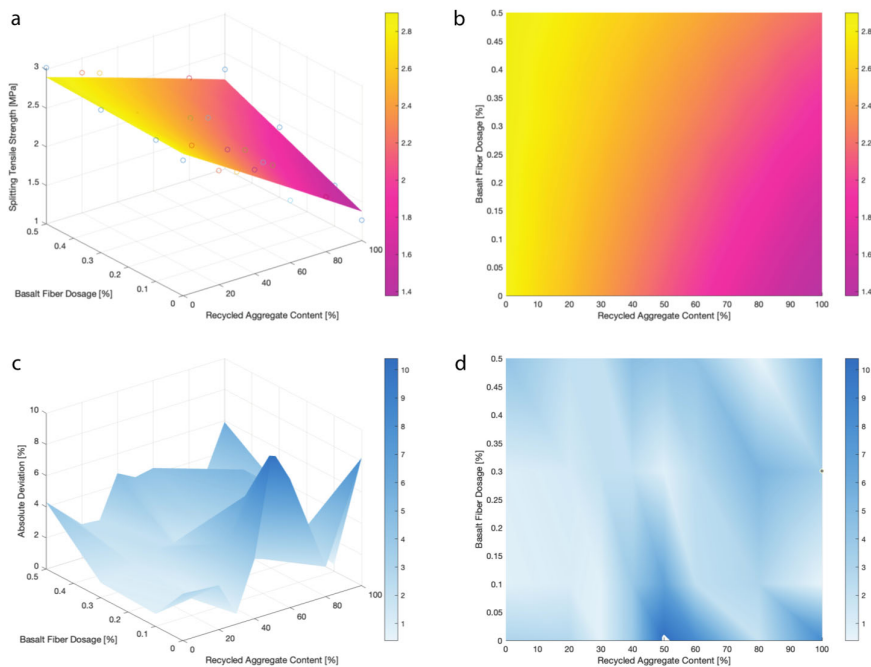


Figure 5. Splitting tensile strength with cubic function: (a) 3D trend surface of splitting tensile strength, (b) contour map of splitting tensile strength, (c) 3D distribution of absolute deviation, and (d) contour map of absolute deviation.

The quadratic polynomial is shown in the following equation:

$$f_t = b_{11} + b_{12} \cdot X + b_{13} \cdot Y + b_{14} \cdot X \cdot Y + b_{15} \cdot X.^2 + b_{16} \cdot Y.^2 \quad (2)$$

where X indicates the matrix of recycled aggregate, and Y indicates the matrix of basalt fiber. The matrix of parameters accommodating b_{1i} ($i = 1-6$) is shown in Table 6.

Table 6. Parameter matrix of the fitted quadratic polynomial of the splitting tensile strength.

b11	b12	b13	b14	b15	b16
2.84	-0.01	0.15	0.01	0.00	-0.03

The cubic polynomial is shown in the following equation:

$$F_t = b_{21} + b_{22} * X + b_{23} * Y + b_{24} * X * Y + b_{25} * X.^2 + b_{26} * Y.^2 + b_{27} * Y * X.^2 + b_{28} * X * Y.^2 + b_{29} * X.^3 + b_{210} * Y.^3 \quad (3)$$

where X indicates the matrix of recycled aggregate, and Y indicates the matrix of basalt fiber. The matrix of parameters accommodating b_{2i} ($i = 1-10$) is shown in Table 7.

Table 7. Parameter matrix of the fitted cubic polynomial of the splitting tensile strength.

b21	b22	b23	b24	b25	b26	b27	b28	b29	b210
2.71	-0.01	1.16	-0.01	0.00	-3.91	0.00	-0.01	0.00	5.75

As shown in Figures 5 and 6, for ordinary concrete, the splitting tensile strength shows an increasing trend with the increase in the basalt fiber dosage. For recycled concrete, when the replacement rate of recycled aggregate is less than 70%, the splitting tensile strength shows a trend of increasing, then decreasing, and then increasing with the increase in the basalt fiber dosage. Firstly, at small dosages, this trend is mainly due to the basalt fibers increasing the adhesion of the concrete, thus causing the tensile strength increase; secondly, at large dosages, this trend is mainly due to the tensile capacity of the basalt fibers themselves [48]. When the replacement rate of recycled aggregate is greater than 70%, with the increase in the number of basalt fibers, the strength first increases and then decreases, but it still is greater than the strength of the unadulterated fiber. This is due to the hydrophilic nature of basalt fibers, as it reduces the amount of water required for cement hydration. It can be seen that the fluctuation in the split tensile strength of recycled concrete with 0.1% fiber dosage tends to flatten out compared to that of recycled concrete without fiber dosage, and it can also be seen that basalt fibers have a very obvious effect on the enhancement of the split tensile strength of concrete with a large replacement rate of recycled aggregates.

Figure 7 shows the reinforcement mechanism of basalt fiber upon the recycled aggregate concrete. The bridging and inhibiting effect of basalt fibers on recycled concrete is divided into three stages [49]. In the first stage, basalt fiber-reinforced recycled concrete formed several tiny cracks and micropores in the curing stage. In the second stage, basalt fibers were randomly distributed in the recycled concrete matrix, showing cross-alignment. The basalt-fiber-cementitious matrix formed a fiber-substrate interface, which limited the development and expansion of the internal microcracks. When the recycled concrete was stressed to the first crack, the basalt fibers bore part of the transverse tensile force, slowing down the stress concentration inside the specimen and effectively preventing the expansion and occurrence of cracks. In this scenario, basalt fiber-reinforced recycled concrete showed good toughness. In the third stage, the specimen was completely crushed, and penetration cracks were formed.

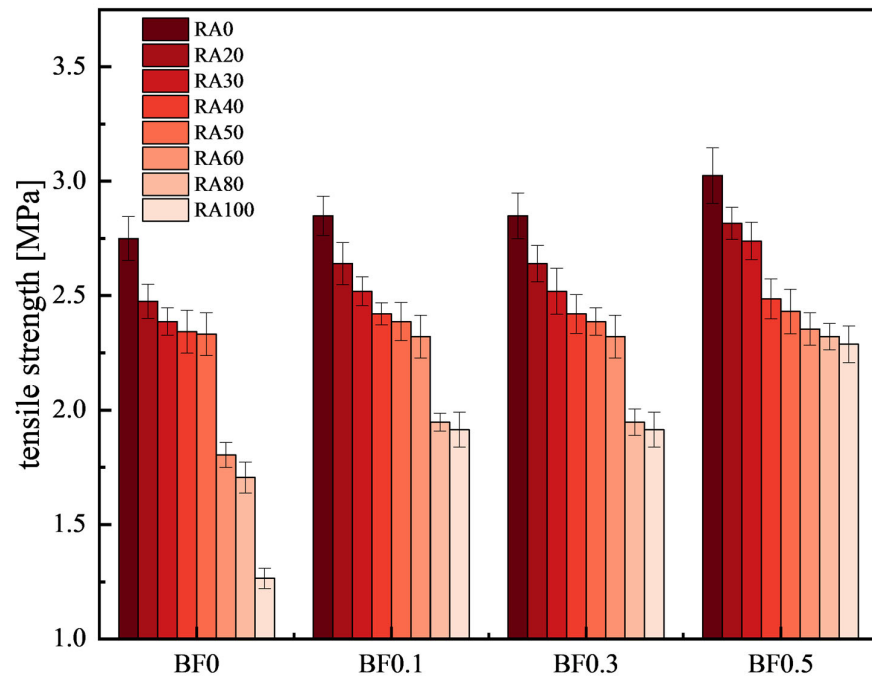


Figure 6. The splitting tensile strength of basalt fiber-reinforced recycled aggregates.

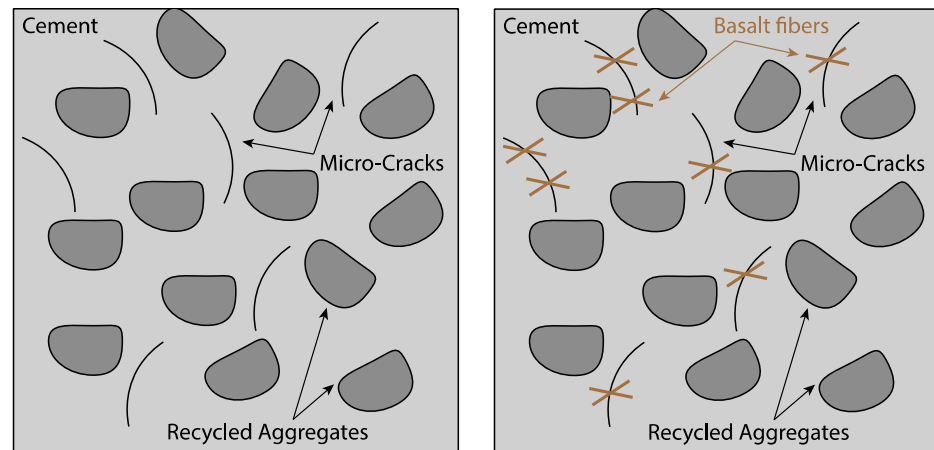


Figure 7. Schematic diagram of enhancement mechanism: without basalt fiber (left) and with basalt fiber (right).

4. Conclusions

This work provides a feasible approach to strengthening recycled aggregate concrete. The basalt fiber as an environmentally friendly fiber in a small dosage effectively lifts the strength of concrete prepared with recycled aggregates. Through the study of basalt fiber-reinforced recycled concrete, the following conclusions can be drawn.

Basalt fibers reduce the fluidity of recycled concrete, increase the friction between the cement matrix, and have a certain enhancement and toughening effect on the cubic compressive strength of recycled concrete and the splitting tensile strength.

Regarding the same fiber admixture, the increase in the replacement rate of recycled coarse aggregate shows a more stable upward trend. Under the same fiber dosage, the increase in the replacement rate of recycled coarse aggregate results in a stable upward trend. The fiber in a dosage of 0.5% makes the compressive strength of concrete prepared with 100% recycled aggregates comparable to that of natural aggregate concrete, whilst achieving a c.a. 90% splitting tensile strength.

For the splitting tensile strength, the fluctuation of the splitting tensile strength of recycled concrete at a 0.1% fiber dosage tends to flatten out, and basalt fibers enhance the splitting tensile strength of concrete with a larger recycled aggregate substitution rate obviously.

Author Contributions: W.-Z.C., conceptualization, measurements and experiments, and draft writing; X.-F.C., writing—review and editing, supervising, and funding acquisition. All authors have read and agreed to the published version of the manuscript.

Funding: This project was financially supported by the Natural Science Foundation of Fujian, grant number 2023J01999; and the Engineering Research Center of Disaster Prevention and Mitigation of Southeast Coastal Engineering Structures of Fujian Province University, grant number 2022001.

Data Availability Statement: Data are contained within the article.

Acknowledgments: Special thanks to the ‘Testing Technology Center for Materials and Devices of Tsinghua Shenzhen International Graduate School’ for providing testing-related service.

Conflicts of Interest: The authors declare no conflict of interest.

References

1. Lu, Z.; Tan, Q.; Lin, J.; Wang, D. Properties investigation of recycled aggregates and concrete modified by accelerated carbonation through increased temperature. *Constr. Build. Mater.* **2022**, *341*, 127813. [[CrossRef](#)]
2. Wang, R.; Zhang, Y.X. Recycling fresh concrete waste: A review. *Struct. Concr.* **2018**, *19*, 1939–1955. [[CrossRef](#)]
3. Chen, X.F.; Jiao, C.J. Experimental Investigation and Modeling of the Sulfur Dioxide Abatement of Photocatalytic Mortar Containing Construction Wastes Pre-Treated by Nano TiO₂. *Catalysts* **2022**, *12*, 708. [[CrossRef](#)]
4. Matar, P.; Assaad, J.J. Concurrent effects of recycled aggregates and polypropylene fibers on workability and key strength properties of self-consolidating concrete. *Constr. Build. Mater.* **2019**, *199*, 492–500. [[CrossRef](#)]
5. Katkhuda, H.; Shatarat, N. Improving the mechanical properties of recycled concrete aggregate using chopped basalt fibers and acid treatment. *Constr. Build. Mater.* **2017**, *140*, 328–335. [[CrossRef](#)]
6. Junak, J.; Sicakova, A. Concrete Containing Recycled Concrete Aggregate with Modified Surface. *Procedia Eng.* **2017**, *180*, 1284–1291. [[CrossRef](#)]
7. Chen, X.F.; Jiao, C.J. A photocatalytic mortar prepared by tourmaline and TiO₂ treated recycled aggregates and its air-purifying performance. *Case Stud. Constr. Mater.* **2022**, *16*, e01073. [[CrossRef](#)]
8. Chen, X.F.; Jiao, C.J. Effect of construction wastes on the rheo-physical behavior of photocatalytic mortar. *Case Stud. Constr. Mater.* **2022**, *16*, e01049. [[CrossRef](#)]
9. Wang, D.; Cui, C.; Chen, X.F.; Zhang, S.; Ma, H. Characteristics of autoclaved lightweight aggregates with quartz tailings and its effect on the mechanical properties of concrete. *Constr. Build. Mater.* **2020**, *262*, 120110. [[CrossRef](#)]
10. Sun, Z.; Li, Y.; Ming, X.; Chen, B.; Li, Z. Enhancing anti-washout behavior of cement paste by polyacrylamide gelation: From flocc properties to mechanism. *Cem. Concr. Compos.* **2023**, *136*, 104887. [[CrossRef](#)]
11. Dong, J.F.; Wang, Q.Y.; Guan, Z.W. Material properties of basalt fibre reinforced concrete made with recycled earthquake waste. *Constr. Build. Mater.* **2017**, *130*, 241–251. [[CrossRef](#)]
12. Guo, H.; Shi, C.; Guan, X.; Zhu, J.; Ding, Y.; Ling, T.C.; Zhang, H.; Wang, Y. Durability of recycled aggregate concrete—A review. *Cem. Concr. Compos.* **2018**, *89*, 251–259. [[CrossRef](#)]
13. Zhou, Y.; Guo, D.; Xing, F.; Guo, M. Multiscale mechanical characteristics of ultra-high performance concrete incorporating different particle size ranges of recycled fine aggregate. *Constr. Build. Mater.* **2021**, *307*, 125131. [[CrossRef](#)]
14. Silva, R.V.; de Brito, J.; Dhir, R.K. Fresh-state performance of recycled aggregate concrete: A review. *Constr. Build. Mater.* **2018**, *178*, 19–31. [[CrossRef](#)]
15. Wang, D.; Wang, H.; Larsson, S.; Benzerzour, M.; Maherzi, W.; Amar, M. Effect of basalt fiber inclusion on the mechanical properties and microstructure of cement-solidified kaolinite. *Constr. Build. Mater.* **2020**, *241*, 118085. [[CrossRef](#)]
16. Dilbas, H.; Çakır, Ö. Influence of basalt fiber on physical and mechanical properties of treated recycled aggregate concrete. *Constr. Build. Mater.* **2020**, *254*, 119216. [[CrossRef](#)]
17. Silva, R.V.; de Brito, J.; Dhir, R.K. Use of recycled aggregates arising from construction and demolition waste in new construction applications. *J. Clean. Prod.* **2019**, *236*, 117629. [[CrossRef](#)]
18. Chen, X.-F.; Jiao, C.-J. Effect of physical properties of construction wastes based composite photocatalysts on the sulfur dioxide degradation: Experimental investigation and mechanism analysis. *Case Stud. Constr. Mater.* **2022**, *17*, e01237. [[CrossRef](#)]
19. Carneiro, J.A.; Lima, P.R.L.; Leite, M.B.; Toledo Filho, R.D. Compressive stress-strain behavior of steel fiber reinforced-recycled aggregate concrete. *Cem. Concr. Compos.* **2014**, *46*, 65–72. [[CrossRef](#)]
20. Théréne, F.; Keita, E.; Naël-Redolfi, J.; Boustingorry, P.; Bonafous, L.; Roussel, N. Water absorption of recycled aggregates: Measurements, influence of temperature and practical consequences. *Cem. Concr. Res.* **2020**, *137*, 106196. [[CrossRef](#)]
21. Shi, C.; Li, Y.; Zhang, J.; Li, W.; Chong, L.; Xie, Z. Performance enhancement of recycled concrete aggregate—A review. *J. Clean. Prod.* **2016**, *112*, 466–472. [[CrossRef](#)]

22. Mistri, A.; Bhattacharyya, S.K.; Dhama, N.; Mukherjee, A.; Barai, S.V. A review on different treatment methods for enhancing the properties of recycled aggregates for sustainable construction materials. *Constr. Build. Mater.* **2020**, *233*, 117894. [[CrossRef](#)]
23. Shaban, W.M.; Yang, J.; Su, H.; Mo, K.H.; Li, L.; Xie, J. Quality improvement techniques for recycled concrete aggregate: A review. *J. Adv. Concr. Technol.* **2019**, *17*, 151–167. [[CrossRef](#)]
24. Wu, C.-R.; Zhu, Y.-G.; Zhang, X.-T.; Kou, S.-C. Improving the properties of recycled concrete aggregate with bio-deposition approach. *Cem. Concr. Compos.* **2018**, *94*, 248–254. [[CrossRef](#)]
25. Yue, G.; Ma, Z.; Liu, M.; Liang, C.; Ba, G. Damage behavior of the multiple ITZs in recycled aggregate concrete subjected to aggressive ion environment. *Constr. Build. Mater.* **2020**, *245*, 118419. [[CrossRef](#)]
26. Jiao, C.-J.; Zhang, X.-C.; Chen, W.-Z.; Chen, X.-F. Mechanical Property and Dimensional Stability of Chopped Basalt Fiber-Reinforced Recycled Concrete and Modeling with Fuzzy Inference System. *Buildings* **2023**, *13*, 97. [[CrossRef](#)]
27. Zeng, W.; Zhao, Y.; Zheng, H.; sun Poon, C. Improvement in corrosion resistance of recycled aggregate concrete by nano silica suspension modification on recycled aggregates. *Cem. Concr. Compos.* **2020**, *106*, 103476. [[CrossRef](#)]
28. Knight, K.A.; Cunningham, P.R.; Miller, S.A. Optimizing supplementary cementitious material replacement to minimize the environmental impacts of concrete. *Cem. Concr. Compos.* **2023**, *139*, 105049. [[CrossRef](#)]
29. Srivastava, S.; Cerutti, M.; Nguyen, H.; Carvelli, V.; Kinnunen, P.; Illikainen, M. Carbonated steel slags as supplementary cementitious materials: Reaction kinetics and phase evolution. *Cem. Concr. Compos.* **2023**, *142*, 105213. [[CrossRef](#)]
30. Rahman, S.M.A.; Dodd, A.; Khair, S.; Shaikh, F.U.A.; Sarker, P.K.; Hosan, A. Assessment of lithium slag as a supplementary cementitious material: Pozzolanic activity and microstructure development. *Cem. Concr. Compos.* **2023**, *143*, 105262. [[CrossRef](#)]
31. Quan, C.-Q.; Jiao, C.-J.; Chen, W.-Z.; Xue, Z.-C.; Liang, R.; Chen, X.-F. The Impact of Fractal Gradation of Aggregate on the Mechanical and Durable Characteristics of Recycled Concrete. *Fractal Fract.* **2023**, *7*, 663. [[CrossRef](#)]
32. Xiao, J.; Ma, Z.; Sui, T.; Akbarnezhad, A.; Duan, Z. Mechanical properties of concrete mixed with recycled powder produced from construction and demolition waste. *J. Clean. Prod.* **2018**, *188*, 720–731. [[CrossRef](#)]
33. Wu, B.; Liu, Y.; Feng, P.; Qiu, J. Cracking can make concrete stronger—The coupled effect of matrix cracking and SiO₂-enhanced fiber/matrix interface healing on the tensile strength of FRCC. *Cem. Concr. Compos.* **2023**, *138*, 105011. [[CrossRef](#)]
34. Shen, D.; Liu, C.; Luo, Y.; Shao, H.; Zhou, X.; Bai, S. Early-age autogenous shrinkage, tensile creep, and restrained cracking behavior of ultra-high-performance concrete incorporating polypropylene fibers. *Cem. Concr. Compos.* **2023**, *138*, 104948. [[CrossRef](#)]
35. Liang, C.; Lu, N.; Ma, H.; Ma, Z.; Duan, Z. Carbonation behavior of recycled concrete with CO₂-curing recycled aggregate under various environments. *J. CO₂ Util.* **2023**, *39*, 101185. [[CrossRef](#)]
36. Gonçalves, T.; Silva, R.V.; de Brito, J.; Fernández, J.M.; Esquinas, A.R. Mechanical and durability performance of mortars with fine recycled concrete aggregates and reactive magnesium oxide as partial cement replacement. *Cem. Concr. Compos.* **2020**, *105*, 103420. [[CrossRef](#)]
37. Xuan, D.; Zhan, B.; Poon, C.S. Assessment of mechanical properties of concrete incorporating carbonated recycled concrete aggregates. *Cem. Concr. Compos.* **2016**, *65*, 67–74. [[CrossRef](#)]
38. Kou, S.-C.; Zhan, B.; Poon, C.-S. Use of a CO₂ curing step to improve the properties of concrete prepared with recycled aggregates. *Cem. Concr. Compos.* **2014**, *45*, 22–28. [[CrossRef](#)]
39. Kazmi, S.M.S.; Munir, M.J.; Wu, Y.F.; Patnaikuni, I.; Zhou, Y.; Xing, F. Axial stress-strain behavior of macro-synthetic fiber reinforced recycled aggregate concrete. *Cem. Concr. Compos.* **2019**, *97*, 341–356. [[CrossRef](#)]
40. Das, C.S.; Dey, T.; Dandapat, R.; Mukharjee, B.B.; Kumar, J. Performance evaluation of polypropylene fibre reinforced recycled aggregate concrete. *Constr. Build. Mater.* **2018**, *189*, 649–659. [[CrossRef](#)]
41. Dimitriou, G.; Savva, P.; Petrou, M.F. Enhancing mechanical and durability properties of recycled aggregate concrete. *Constr. Build. Mater.* **2018**, *158*, 228–235. [[CrossRef](#)]
42. Zhang, C.; Wang, Y.; Zhang, X.; Ding, Y.; Xu, P. Mechanical properties and microstructure of basalt fiber-reinforced recycled concrete. *J. Clean. Prod.* **2021**, *278*, 123252. [[CrossRef](#)]
43. Alnahhal, W.; Aljidda, O. Flexural behavior of basalt fiber reinforced concrete beams with recycled concrete coarse aggregates. *Constr. Build. Mater.* **2018**, *169*, 165–178. [[CrossRef](#)]
44. Wang, Y.; Hughes, P.; Niu, H.; Fan, Y. A new method to improve the properties of recycled aggregate concrete: Composite addition of basalt fiber and nano-silica. *J. Clean. Prod.* **2019**, *236*, 117602. [[CrossRef](#)]
45. Li, Z.-X.; Li, C.-H.; Shi, Y.-D.; Zhou, X.-J. Experimental investigation on mechanical properties of Hybrid Fibre Reinforced Concrete. *Constr. Build. Mater.* **2017**, *157*, 930–942. [[CrossRef](#)]
46. Algin, Z.; Ozen, M. The properties of chopped basalt fibre reinforced self-compacting concrete. *Constr. Build. Mater.* **2018**, *186*, 678–685. [[CrossRef](#)]
47. High, C.; Seliem, H.M.; El-Safty, A.; Rizkalla, S.H. Use of basalt fibers for concrete structures. *Constr. Build. Mater.* **2015**, *96*, 37–46. [[CrossRef](#)]

48. Zheng, Y.; Zhuo, J.; Zhang, P.; Ma, M. Mechanical properties and meso-microscopic mechanism of basalt fiber-reinforced recycled aggregate concrete. *J. Clean. Prod.* **2022**, *370*, 133555. [[CrossRef](#)]
49. Zhang, X.; Zhou, G.; Xu, P.; Fu, L.; Deng, D.; Kuang, X.; Fan, Y. Mechanical Properties under Compression and Microscopy Analysis of Basalt Fiber Reinforced Recycled Aggregate Concrete. *Materials* **2023**, *16*, 2520. [[CrossRef](#)]

Disclaimer/Publisher's Note: The statements, opinions and data contained in all publications are solely those of the individual author(s) and contributor(s) and not of MDPI and/or the editor(s). MDPI and/or the editor(s) disclaim responsibility for any injury to people or property resulting from any ideas, methods, instructions or products referred to in the content.